Detrainment in deep convection

S. J. Böing,[1] A. P. Siebesma,[1,2] J. D. Korpershoek,[1] and H. J. J. Jonker[1]

Received 30 August 2012; revised 3 October 2012; accepted 4 October 2012; published 31 October 2012.

[1] This study explores the mechanisms that determine detrainment in deep cumulus convection. A set of 90 high-resolution Large Eddy Simulations is used to systematically explore the sensitivity of continental deep convection to the relative humidity and stability of the free troposphere. It appears that variations in the mass-flux profiles are determined by detrainment, rather than entrainment. The detrainment shows a strong dependence on the critical mixing ratio, a dimensionless parameter which describes which mixtures of cloud core and environmental air are positively buoyant. A conceptual approach to the parameterization of detrainment is proposed on the basis of these results. **Citation:** Böing, S. J., A. P. Siebesma, J. D. Korpershoek, and H. J. J. Jonker (2012), Detrainment in deep convection, *Geophys. Res. Lett.*, *39*, L20816, doi:10.1029/2012GL053735.

1. Introduction

[2] The parameterization of cumulus convection is a key challenge in improving the performance of Numerical Weather Prediction (NWP) and climate models, in particular in the tropics. The formulation of convection schemes has a large impact on phenomena such as the Madden-Julian Oscillation [*Zhang and Mu*, 2005; *Lin et al.*, 2006], the structure and location of the Intertropical Convergence Zone [*Frey and Latif*, 1997; *Liu et al.*, 2010] and the diurnal cycle over land [*Yang and Slingo*, 2001; *Bechtold et al.*, 2004]. Moreover, the parametric assumptions on the mixing between convective clouds and their environment have been shown to be a main source in climate model uncertainty [*Murphy et al.*, 2004].

[3] Most convection schemes are based on a bulk-plume approach, where the parameterization describes the behavior of the ensemble of clouds that are actively contributing to the transport of heat, moisture and momentum. The intensity and vertical extent of the moist convection is described by the mass-flux $M_c = \rho a_c w_c$, with a_c denoting the fractional area of the cloud core, w_c its vertical velocity and ρ the density. The behavior of the mass-flux is governed by the (fractional) entrainment and detrainment rates, ϵ and δ, which represent the mixing of environmental air into the cloud core and the removal of air that no longer contributes to updrafts:

$$\frac{1}{M_c}\frac{d}{dz}M_c = \epsilon - \delta \tag{1}$$

The sensitivity of deep convection to the relative humidity in the free troposphere has been the topic of many recent studies. Both observations [*Holloway and Neelin*, 2009] and Cloud Resolving Model (CRM) simulations [*Derbyshire et al.*, 2004; *Waite and Khouider*, 2010] show that besides stability, a dry environment can be a key inhibiting factor for the development of deep clouds. More detailed Large Eddy Simulation (LES) studies [*De Rooy and Siebesma*, 2008] showed that a dryer environment promotes stronger detrainment rates for shallow cumulus convection, a finding that was more recently confirmed in CRM studies of deep convection [*Derbyshire et al.*, 2011; *De Rooy et al.*, 2012].

[4] Most convection parameterizations fail to show any significant sensitivity to the free tropospheric humidity [*Derbyshire et al.*, 2004]. In an attempt to rectify this, *Bechtold et al.* [2008] proposed to make the entrainment an explicit function of the environmental relative humidity, such that entrainment decreases in a moister environment. This has been shown to improve the performance of the global NWP model used at the European Center for Medium-Range Weather Forecasts (ECMWF).

[5] One existing bulk-plume scheme that intrinsically incorporates the sensitivity of convection to its environment was developed by *Kain and Fritsch* [1990]. The scheme is based on the assumption that at the interface of the cloud core and the environment, a certain mass of cloud core air m_c mixes with a mass m_e of air with the properties of the mean environment (the subscripts c and e will be used throughout this article). The mixtures that result can be described in terms of a mixing ratio χ, which indicates the fraction of environmental air in the mixture.

[6] The key idea behind the Kain-Fritsch scheme is that positively buoyant mixtures entrain into the cloud core, whereas mixtures that become negatively buoyant due to evaporative cooling (having $\chi > \chi_{cr}$) are detrained. Assuming all mixing ratios occur with equal probability $p(\chi)$, the entrainment and detrainment rates can be analytically expressed in terms of χ_{cr} [*Bretherton and McCaa*, 2004]:

$$\epsilon = \frac{2}{\lambda}\int_0^{\chi_{cr}} \chi p(\chi) d\chi = \frac{\chi_{cr}^2}{\lambda} \tag{2}$$

$$\delta = \frac{2}{\lambda}\int_{\chi_{cr}}^{1} (1-\chi)\, p(\chi) d\chi = \frac{(1-\chi_{cr})^2}{\lambda} \tag{3}$$

$$\delta - \epsilon = \frac{1}{\lambda}(1 - 2\chi_{cr}) \tag{4}$$

Here, λ is a length scale for the mixing of the cloud core with its environment.

[7] *De Rooy and Siebesma* [2008, equation (A9)] showed that χ_{cr} increases with higher relative humidity and with

[1]Department of Multi-scale Physics, Delft University of Technology, Delft, Netherlands.
[2]Royal Netherlands Meteorological Institute, De Bilt, Netherlands.

Corresponding author: S. J. Böing, Department of Multi-scale Physics, Delft University of Technology, PO Box 5048, NL-2600 GA Delft, Netherlands. (s.j.boing@tudelft.nl)

0094-8276/12/2012GL053735

higher buoyancy excess of the cloud core, which in turn depends on the stability. A fundamental problem with the formulation (equation (2)) is that it predicts a decreasing entrainment rate (which results in larger moisture excesses) in a drier environment, in clear disagreement with the CRM/LES results and proposed parameterization discussed above.

[8] In the current work, we will systematically determine the relative dependency of entrainment, detrainment and the intensity moist convection in general on humidity, stability and the critical mixing ratio χ_{cr}. This will be done by a massive sensitivity study of 90 three-dimensional Large Eddy Simulations of deep convection.

2. Sensitivity Experiments and Results

[9] The simulations are performed using the Dutch Atmospheric Large Eddy Simulation (DALES) Model. For the details of the code, the reader is referred to *Heus et al.* [2010] with the modifications described in *Böing et al.* [2012]. The simulations were executed on a $57.6 \times 57.6 \times 25$ km domain with a resolution of 150 m in the horizontal, while the vertical resolution varied from 40 m near the surface to 150 m near the tropopause.

[10] Our case setup is similar to the two-dimensional sensitivity experiment of *Wu et al.* [2009], which was an idealization of a CRM intercomparison study of the diurnal cycle in North-West Brazil [*Grabowski et al.*, 2006].

[11] The different initial stability and relative humidity profiles that span the phase space explored in this study can be found in the auxiliary material.[1] The main added value of the new simulations as compared to those of *Wu et al.* [2009] is that they span a wider range of relative humidities and stabilities and that they are truly 3-dimensional. The initial surface temperature is 295.4 K. A shear of 4 ms^{-1} over the lower 5 km is enforced. Following *Wu et al.* [2009] the sensible and latent heat fluxes are prescribed (161 and 343 Wm^{-2} respectively) and no radiative tendencies are applied. Though we realise that these are severe simplifications, we think that they will not affect the nature of the dependencies of the convection on the environmental conditions that will be explored in this paper.

[12] In order to analyze the entrainment rate, the buoyant cloud core decomposition is used as a sampling criterion ($\theta_v > \overline{\theta_v}$ and $q_l > 0$, with θ_v denoting the virtual potential temperature and the overline a horizontal mean). The entrainment rate is diagnosed from the budget equation of a scalar variable ϕ, using a cloud core decomposition [*Siebesma and Cuijpers*, 1995]. A top-hat approach gives:

$$\rho a_c \frac{\partial}{\partial t}\phi_c = -M_c \epsilon_\phi (\phi_c - \phi_e) - M_c \frac{\partial}{\partial z}\phi_c + \rho a_c \frac{\partial}{\partial t}\phi_c|_S \quad (5)$$

We thus diagnose the effective entrainment rate that needs to be incorporated in a bulk-plume scheme in order to obtain the correct profiles of ϕ given the mass-flux. The entrainment rate is calculated by inverting the equation (neglecting the left hand side). The last term on the right hand side accounts for local sources and sinks of ϕ. Bulk-plume schemes are often used in operational models, although some recent work has pointed out limitations to their applicability [*Romps*, 2011; *Dawe and Austin*, 2011]. The success of a bulk-plume approach depends on its ability to capture the transport of at least heat and moisture.

[13] We use total water specific humidity (q_t) as the scalar variable, hence the sources and sinks are due to microphysics. The advantage of using q_t is that its cloud core value decreases rapidly with height, resulting in a more robust behavior of ϵ. The detrainment rate δ itself is diagnosed using ϵ and the mass-flux (equation (1)). We will perform our analyses on the 8th hour of simulation, since by that time the mass-fluxes, entrainment and detrainment do not show any strong dependencies with time anymore. The system has not reached a true steady state, as the environmental profiles change only on much longer time scales, but the entrainment and detrainment rates in the lower troposphere have adjusted to the environment. Figure 1 shows six vertical profiles of the diagnosed entrainment and detrainment rates averaged over the 8th hour for a low, a medium and a high relative humidity environment combined with a high and a low stability.

[14] A number of observations can be made. First of all, deeper and stronger convection is promoted by a more unstable but also by a more humid atmosphere. The entrainment, however, appears to be rather insensitive to the environmental conditions and decreases with height for all cases in a similar way (approximately proportional to $1/z$). The detrainment, on the other hand, increases strongly in a dryer and a more stable environment. As a result, the difference between detrainment and entrainment is maximal for the dry stable cases, leading to a strongly decreasing mass-flux with height (equation (1)). In the moist unstable cases, however, the mass-flux profile is almost constant with height. From these results we conclude that the mass-flux profile is mainly governed by the detrainment, as was also found for shallow cumulus convection [*De Rooy and Siebesma*, 2008].

[15] In order to further explore the dependencies of convection on the environment we show in Figure 2 the various characteristics of the moist convection at 2500 m above ground level. This level is used for all simulations; note that the cloud base is at a similar level, possibly due to the fact that the initial relative humidity in the boundary layer is kept constant (see Figure S1). The axes show the initial stability near the surface and the initial free tropospheric relative humidity. Figures 2a and 2b show the entrainment and detrainment rates on the same scale, further strengthening the conclusion that the variation of the mass-flux is largely governed by detrainment. Only if we display the entrainment on a much smaller scale (Figure 2c), can it be observed that also the entrainment rates decrease in a moister and more unstable atmosphere. The changes in other measures of convective activity such as cloud top height and precipitation rate (Figures 2d and 2e) show a similar behaviour: higher cloud tops and more precipitation occur in a moister and more unstable atmosphere. Cloud top height is diagnosed as the height at which the mass-flux has decreased to 1% of its maximum value. Finally, the critical mixing χ_{cr} diagnosed at 2500 m (Figure 2f) also shows a similar dependence on the environmental conditions, with typical values of χ_{cr} around 0.2–0.3.

3. A Simple Model for the Mass-Flux

[16] The results from the previous section suggest a strong correlation between the detrainment δ and χ_{cr}. In order to further explore this relationship, we show in Figures 3a–3c the diagnosed entrainment and detrainment rates as well as

[1] Auxiliary materials are available in the HTML. doi:10.1029/2012GL053735.

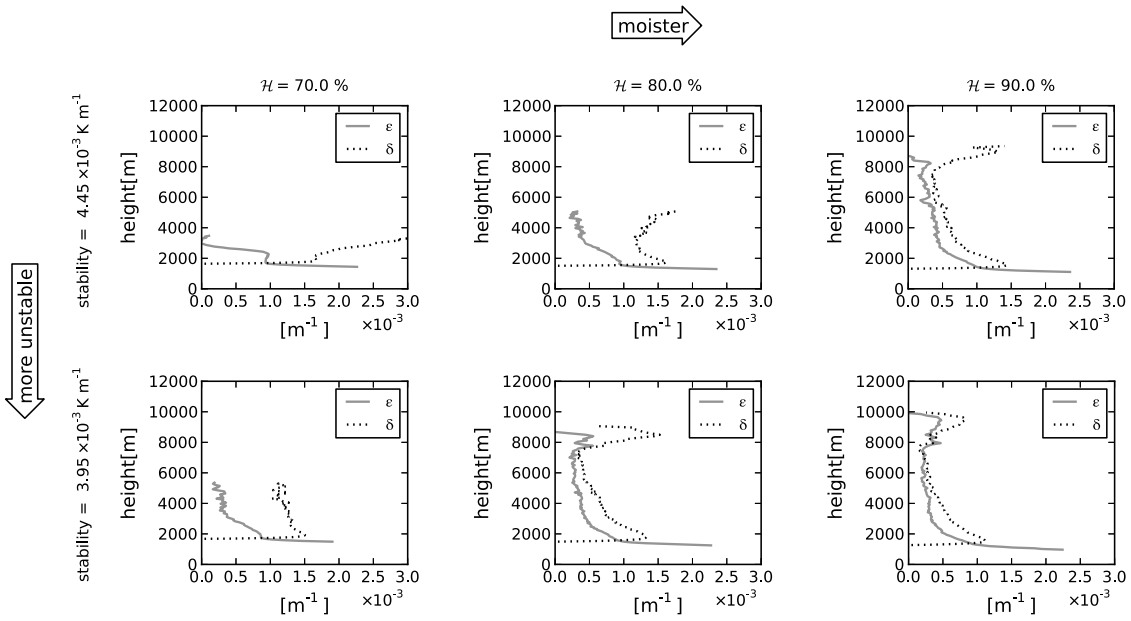

Figure 1. Variations of entrainment and detrainment rates of q_t as a function of the initial stability (virtual potential temperature lapse rate at the surface) and relative humidity. Statistics are sampled during the 8th hour of the simulations. Only levels where the mass-flux is more than 5 % of its cloud base value are shown.

their difference as a function of χ_{cr} for all 90 simulations at model levels below 6000 m.

[17] The entrainment rates (Figure 3a) do not show a consistent dependence on χ_{cr} at each height, although a weak dependence in the bulk values is found. However, this dependence is much weaker than the clear decrease with height that is found. The detrainment rates (Figure 3b), however, do show a clear relation with χ_{cr} at every height, though also here a systematic decrease with height is present. The difference $\delta - \epsilon$ (Figure 3c), which determines the shape of the mass-flux profile (see equation (1)), shows an even better relationship with χ_{cr}. Its overall shape is predominantly determined by detrainment, with only a minor dependence on height. For comparison, Figures 3d and 3e also show the dependence of $\delta - \epsilon$ on relative humidity and stability separately. There is much more scatter on these latter plots, indicating that χ_{cr} is a superior indicator for the combined effect of stability and humidity on convection.

[18] In order to establish a simple parameterization, we use a bulk approach (following *De Rooy and Siebesma* [2008]). We consider the average values of χ_{cr} and $\delta - \epsilon$ over the lower half of the cloud, with cloud top defined as in

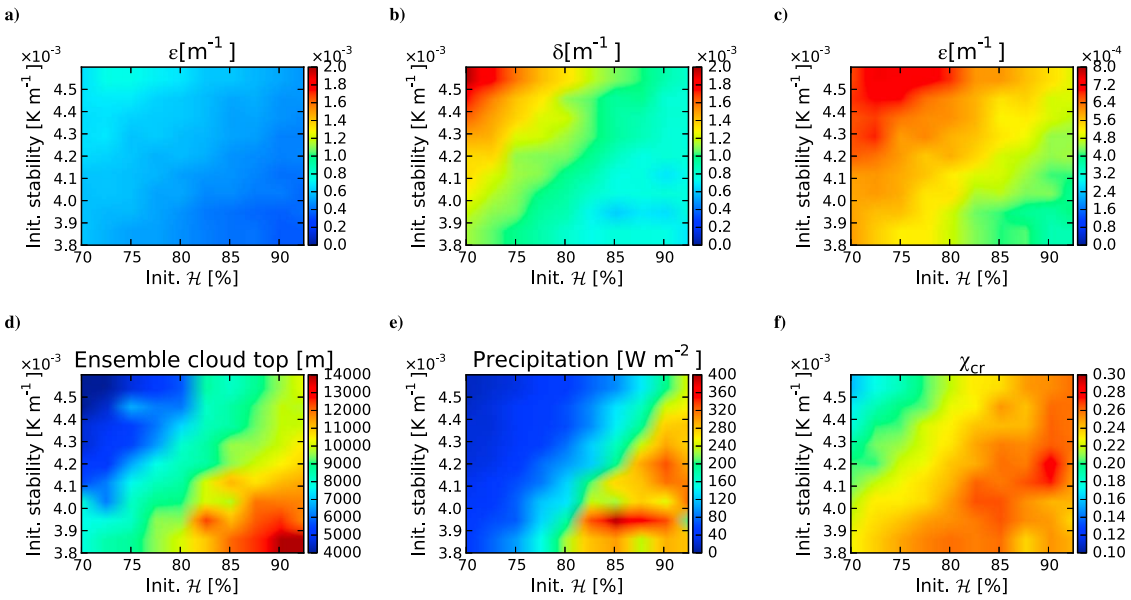

Figure 2. Dependence of (a) ϵ_{q_t}, (b) δ_{q_t}, (c) ϵ_{q_t} (using a smaller color scale), (d) cloud top, (e) precipitation rate and (f) χ_{cr} on the initial relative humidity and stability. ϵ, δ and χ_{cr} are plotted at 2500 meters above ground level. Statistics are sampled during the 8th hour of the simulation.

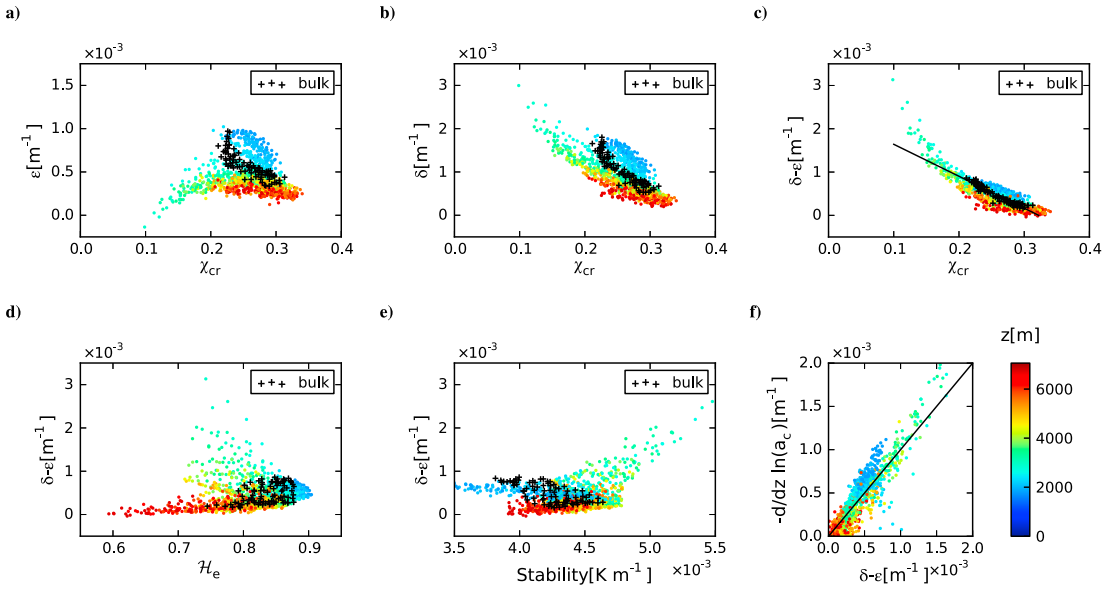

Figure 3. (a–c) Dependence of ϵ, δ, and $\delta - \epsilon$ on χ_{cr}. (d, e) Dependence of $\delta - \epsilon$ on relative humidity and virtual potential temperature lapse rate (at the same time) during the 8th hour of the simulation. (f) Correlation between $\delta - \epsilon$ and fractional decrease in a_c. Crosses are mean values over the lower half of the cloud, the line in panel c corresponds to equation (7). Color indicates the height where statistics are sampled.

the previous section. The results are shown as black crosses in Figure 3. We are now in a position to compare these results with equations (2)–(4). We do not find a pronounced relation between ϵ and χ_{cr} , contradicting equation (2). The detrainment δ and hence also $\delta - \epsilon$ do show a strong dependence on χ_{cr}. However, $\delta - \epsilon$ becomes small at relatively low values of χ_{cr} (around 0.3, as in *De Rooy and Siebesma* [2008], whereas Kain-Fritsch predicts $\delta - \epsilon = 0$ for $\chi_{cr} = 0.5$). The small values of χ_{cr} are due to relatively small buoyancy excesses of the cloud core in the LES.

[19] In order to find a physical interpretation of the results, we investigate whether the changes in the gradient of the mass-flux should be attributed to changes in cloud fraction or to changes in the vertical velocity, using the relation

$$\delta - \epsilon = -\frac{d}{dz}\ln M_c = -\frac{d}{dz}\ln \rho - \frac{d}{dz}\ln a_c - \frac{d}{dz}\ln w_c \qquad (6)$$

Virtually all the differences of the mass-flux profiles are caused by changes in the fractional area of the cloud core (see Figure 3f), as was also found for shallow cumulus convection [*Neggers et al.*, 2009; *De Rooy and Siebesma*, 2010]. The physical picture emerging from this is that in the dry stable regime the cloud field is dominated by shallow clouds. As a result, the cloud core fraction and mass-flux are strongly decreasing with height. In the case of moister and more unstable conditions, on the other hand, many of the convective towers are able to reach the upper troposphere.

[20] For a parameterization it is important to realize that a perfect entrainment model predicts the correct value of χ_{cr}. Here. we explore this pathway by assuming that we have the perfect entrainment model, i.e. using the diagnosed values of χ_{cr} from the LES. For simplicity, we use a linear fit to the bulk values (black crosses in Figure 3c) in order to parameterize the dependence:

$$\delta - \epsilon = a - b\chi_{cr} \qquad (7)$$

with $a = 2.4 \times 10^{-3}$ m^{-1} and $b = 7.4 \times 10^{-3}$ m^{-1}. We apply this bulk fit to the local diagnosed value of $\chi_{cr}(z)$ in order to parameterize the mass-flux profiles.

[21] The overall behavior of the 90 simulations seems to be well captured, probably better than any existing convection scheme (Figure 4). The height of the deepest clouds is somewhat underestimated in most cases. Possibly, besides χ_{cr}, the cloud width also plays a role in setting ϵ and δ [*Grabowski et al.*, 2006; *Stirling and Stratton*, 2011]. At the higher

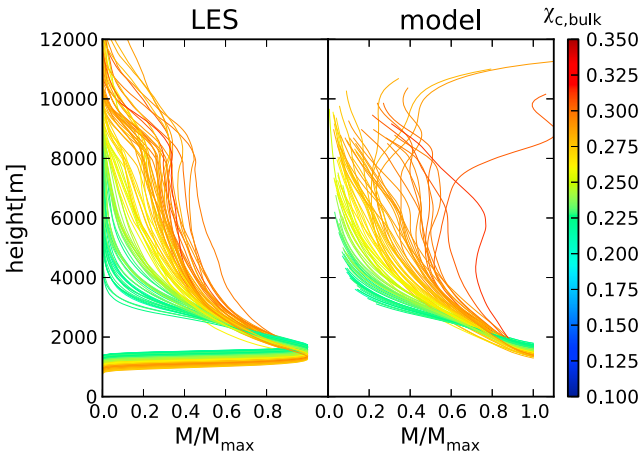

Figure 4. LES mass-flux profiles and semi-prognostic parameterization of the mass-flux using the maximum mass-flux, the profile of χ_{cr} and equation (7).

levels, the smaller and narrower clouds have disappeared from the ensemble [*Böing et al.*, 2012]. This width dependence is also important to take into account if we extend our results to shallow convection. Similar plots as Figure 3 for shallow cumulus cases, such as BOMEX, show that a strong correlation between χ_{cr} and $\delta - \epsilon$ is robust. However, both ϵ and δ tend to have higher values in shallow convection, which is consistent with lower entrainment and detrainment rates for deep convection in other parameterizations [e.g., *Bechtold et al.*, 2001]. Nevertheless, the first order estimates of the mass-fluxes displayed in Figure 4 are highly encouraging.

4. Conclusions

[22] We have investigated an ensemble of 90 cases with deep convection, which shows detrainment depends strongly on the relative humidity and stability of the free troposphere. The mass-flux is governed mainly by detrainment, and a strong correlation between $\delta - \epsilon$ and the critical mixing fraction was found. This dependence also manifests itself in the cloud top height and precipitation rates mainly depending on χ_{cr}. The relationship between the entrainment rate and χ_{cr} is much weaker and has the opposite sensitivity to the *Kain and Fritsch* [1990] scheme, but $1/z$ behaviour seems to hold to first order.

[23] Some recent work [e.g., *Bechtold et al.*, 2008] has focused on the sensitivity of entrainment to relative humidity. The LES results indicate this sensitivity is relatively weak. Nevertheless, subtle differences in entrainment rate may be relevant in determining χ_{cr}. This sensitivity makes an accurate description of the bulk-plume entrainment, as discussed in, e.g., *Grabowski et al.* [2006], important for the success of a fully prognostic parameterization. Assuming such a description is available, Figure 4 shows that direct modelling of the mass-flux using χ_{cr} is a viable approach for the parameterization of deep convection. As an obvious next step we intend to evaluate the present ideas fully prognostically in Single Column Model versions of weather and climate models.

[24] **Acknowledgments.** The use of supercomputer facilities was sponsored by the National Computing Facilities Foundation (NCF), with financial support from NWO. The authors wish to thank Zhiming Kuang and one anonymous reviewer for their valuable comments.

[25] The Editor thanks Zhiming Kuang and an anonymous reviewer for their assistance in evaluating this paper.

References

Bechtold, P., E. Bazile, F. Guichard, P. Mascart, and E. Richard (2001), A mass-flux convection scheme for regional and global models, *Q. J. R. Meteorol. Soc.*, *127*, 869–886.

Bechtold, P., J.-P. Chaboureau, A. Beljaars, A. K. Betts, M. Köhler, M. Miller, and J.-L. Redelsperger (2004), The simulation of the diurnal cycle of convective precipitation over land in a global model, *Q. J. R. Meteorol. Soc.*, *130*, 3119–3137.

Bechtold, P., M. Kohler, T. Jung, F. Doblas-Reyes, M. Leutbecher, M. J. Rodwell, F. Vitart, and G. Balsamo (2008), Advances in simulating atmospheric variability with the ECMWF model: From synoptic to decadal time-scales, *Q. J. R. Meteorol. Soc.*, *134*, 1337–1351.

Böing, S. J., H. J. J. Jonker, A. P. Siebesma, and W. W. Grabowski (2012), Influence of the subcloud layer on the development of a deep convective ensemble, *J. Atmos. Sci.*, *69*(9), 2682–2698.

Bretherton, C. S., and J. R. McCaa (2004), Parameterization for shallow cumulus convection and its application to marine subtropical cloud-topped boundary layers. Part I: Description and 1D results, *Mon. Weather Rev.*, *132*, 864–882.

Dawe, J. T., and P. H. Austin (2011), The influence of the cloud shell on tracer budget measurements of LES cloud entrainment, *J. Atmos. Sci.*, *68*(12), 2909–2920.

De Rooy, W. C., and A. P. Siebesma (2008), A simple parameterization for detrainment in shallow cumulus, *Mon. Weather Rev.*, *136*, 560–576, doi:10.1175/2007MWR2201.1.

De Rooy, W. C., and A. P. Siebesma (2010), Analytical expressions for entrainment and detrainment in cumulus convection, *Q. J. R. Meteorol. Soc.*, *136*, 1216–1227.

De Rooy, W., P. Bechtold, K. Froehlich, C. Hohenegger, H. J. J. Jonker, D. Mironov, A. P. Siebesma, J. Teixeira, and J. Yano (2012), Entrainment and detrainment in cumulus convection: An overview, *Q. J. R. Meteorol. Soc.*, doi:10.1002/qj.1959, in press.

Derbyshire, S. H., I. Beau, P. Bechtold, J. Grandpeix, J.-M. Piriou, J.-L. Redelsperger, and P. M. M. Soares (2004), Sensitivity of moist convection to environmental humidity, *Q. J. R. Meteorol. Soc.*, *130*(604), 3055–3079, doi:10.1256/qj.03.130.

Derbyshire, S. H., A. V. S. Maidens, R. Milton, S. R. A., and M. R. Willett (2011), Adaptive detrainment in a convective parametrization, *Q. J. R. Meteorol. Soc.*, *137*, 1856–1871, doi:10.1002/qj.875.

Frey, H., and M. Latif (1997), The coupled GCM ECHO-2. Part I: The tropical Pacific, *Mon. Weather Rev.*, *125*, 703–720.

Grabowski, W. W., et al. (2006), Daytime convective development over land: A model intercomparison based on LBA observations, *Q. J. R. Meteorol. Soc.*, *132*(615), 317–344.

Heus, T., et al. (2010), Formulation of and numerical studies with the Dutch Atmospheric Large-Eddy Simulation (DALES), *Geosci. Model Dev.*, *3*, 99–180.

Holloway, C. E., and J. D. Neelin (2009), Moisture vertical structure, column water vapor, and tropical deep convection, *J. Atmos. Sci.*, *66*(6), 1665–1683.

Kain, J. S., and J. M. Fritsch (1990), A one-dimensional entraining/detraining plume model and its application in convective parameterization., *J. Atmos. Sci.*, *47*, 2784–2802.

Lin, J.-L., et al. (2006), Tropical intraseasonal variability in 14 IPCC AR4 climate models. Part I: Convective signals, *J. Clim.*, *19*, 2665–2690, doi:10.1175/JCLI3735.1.

Liu, Y., L. Guo, and G. Wu (2010), Sensitivity of ITCZ configuration to cumulus convective parameterizations on an aqua planet, *Clim. Dyn.*, *34*, 223–240.

Murphy, J., D. Sexton, D. Barnett, G. Jones, M. Webb, M. Collins, and D. Stainforth (2004), Quantification of modelling uncertainties in a large ensemble of climate change simulations, *Nature*, *429*, 768–772.

Neggers, R. A. J., M. Köhler, and A. C. M. Beljaars (2009), A dual mass flux framework for boundary layer convection. Part I: Transport, *J. Atmos. Sci.*, *66*(6), 1465–1487.

Romps, D. M. (2011), A direct measure of entrainment, *J. Atmos. Sci.*, *67*(6), 1908–1927.

Siebesma, A. P., and J. Cuijpers (1995), Evaluation of parametric assumptions for shallow cumulus convection, *J. Atmos. Sci.*, *52*(6), 650–666.

Stirling, A. J., and R. A. Stratton (2011), Entrainment processes in the diurnal cycle of deep convection over land, *Q. J. R. Meteorol. Soc.*, *138*, 1135–1149, doi:10.1002/qj.1868.

Waite, M. L., and B. Khouider (2010), The deepening of tropical convection by congestus preconditioning, *J. Atmos. Sci.*, *67*(8), 2601–2615, doi:10.1175/2010JAS3357.1.

Wu, C., B. Stevens, and A. Arakawa (2009), What controls the transition from shallow to deep convection?, *J. Atmos. Sci.*, *66*(6), 1793–1806, doi:10.1175/2008JAS2945.1.

Yang, G., and J. M. Slingo (2001), The diurnal cycle in the tropics, *Mon. Weather Rev.*, *129*, 784–801.

Zhang, G. J., and M. Mu (2005), Simulation of the Madden-Julian Oscillation in the NCAR CCM3 using a revised Zhang-McFarlane convection parameterization scheme, *J. Clim.*, *18*, 4046–4064.